Polypyrrole/oligonucleotide nanocomposite film: steric effect on DNA hybridization

J-H Jiang[1]*, **Y Li**[1,2], **J Wang**[1], and **K-L Paul Sung**[1,3]

[1]Key Laboratory of Biorheological Science and Technology, Chongqing University, Chongqing, People's Republic of China

[2]Central Laboratory of Yongchuan Hospital, Chongqing Medical University, Chongqing, People's Republic of China

[3]Departments of Bioengineering and Orthopedic Surgery, University of California, San Diego, California, USA

The manuscript was received on 21 March 2011 and was accepted after revision for publication on 26 May 2011.

DOI: 10.1177/1740349911413956

Abstract: This paper presents evidence and some preliminary explanation for the existence of a steric effect in polypyrrole/oligonucleotide (PPy/ODN) nanocomposite film, which may be responsible for the high electrochemical sensing performance of that nanofilm when being used in DNA hybridization detection. When hybridization occurs in this nanocomposite film, the steric effect in the immediate interface of the hybrid film can damp the ion-flux penetrating through this interface, thus resulting in the signal differentiation on the electrode electrochemical property. Electrochemical cyclic voltammetry (CV) combined with atomic force microscope (AFM) were utilized to clarify the hindering mechanism occurring on such interface. Furthermore, the hybridization reaction of ODN probes in the hybrid PPy/ODN film with their complementary DNA sequences was measured via CV, with the target ODN concentrations as low as 5×10^{-18} mol/L. Under optimized hybridization conditions the sensor response was almost linear, with the logarithm of the target ODN concentration ranging from 1×10^{-18} to 1×10^{-11} mol/L. These results may be useful in the development of a much simpler label-free DNA sensor based on the PPy/ODN nanocomposite film.

Keywords: DNA, hybridization, polypyrrole, steric effect, cyclic voltammetry, label-free

1 INTRODUCTION

The development of an analytical device capable of identifying specific DNA sequences in a fast, simple, and low-cost manner from the clinical sample has attracted considerable attention from many research groups and high technology companies. In this regard, the electrochemical DNA biosensor, which commonly relies on the hybridization reaction between the DNA target sequences in solution with the ODN probes immobilized on a conducting transducer surface, has become one of the more enabling techniques in the progress towards high sensitivity, low cost, ease of use, and especially in relation to the potential of miniaturization and automation [**1**–**3**].

Currently, the electrochemical DNA biosensor can be established through two approaches: indirect (label-dependent) and direct (label-free), depending on whether there is a need to introduce electrochemical labels (indicators) or not. With the indirect route, some DNA-intercalating molecules, such as Hoechst 33258 [**4**] and methylene blue [**5**], are often employed for the indicator of sequence-specific hybridization event, due to their possession of a much higher affinity to the resulting hybrid. Some good redox labels such as enzyme [**6**], cationic metal complexes [**7**], and nanoparticles [**8**, **9**] have been also utilized in such a way for DNA hybridization detection. Despite the relatively good detection

*Corresponding author: Key Laboratory of Biorheological Science and Technology, Ministry of Education, Bioengineering College, Chongqing University, Chongqing, 400044, People's Republic of China.
email: jhuan@cqu.edu.cn

Downloaded from pin.sagepub.com at NATIONAL UNIV SINGAPORE on August 7, 2011

sensitivity and low detection limit, these label-dependent approaches have shortcomings of high cost, longer manufacture time, and sophisticated operation procedure [**10**]; moreover, the excess of labels can introduce some interference, such as affecting kinetics behaviour in the case of DNA hybridization or changing the binding properties of the labelled DNA target sequences [**11**]. In comparison, the label-free DNA electrochemical biosensor is becoming more attractive, as it overcomes the above-mentioned weak points [**12**, **13**].

As demonstrated in the literature, the realization of 'label-free' routes for electrochemical DNA biosensors is largely through the electrical read-out of signal transformation from the DNA hybridization event to the electrode where the hybridization is occurring [**14**, **15**]. A key question is how to form an effective coupling interface while presenting the hybridization signal between nucleic acid bio-recognition system and electronic transducer system. In fact, polypyrrole (PPy), a classical conjugated conducting polymer, holds particular promise for meeting such requirements to a large extent. It has been reported that ODN probes could be grafted or absorbed on polypyrrole film and that the changes in the electrochemical properties of the film once DNA hybridization had occurred could be measured [**16**–**19**]. ODN probes, especially, could serve as the sole dopant during PPy electrochemical polymerization, and maintain their hybridization activity and affinity to target sequences within the host PPy network, as already revealed by Wang [**20**, **21**]. Based on these facts, Cai *et al.* reported an indicator-free DNA hybridization detection strategy via impedance measurement on carbon nanotube-modified electrode [**14**], and that the detection limit could be decreased further when combined with the metallization of the helix DNA after hybridization [**22**]. More interestingly, a more direct electrochemical sensor for fast reagent-free DNA detection has been developed by chrono-amperometry [**23**]. Recently, Tosar *et al.* [**24**] reported an electrochemical DNA biosensor system, which contains two independent direct detection methods for enhancing the specificity of this biosensor system. As for the interpretation for the signal transduction mechanism in such PPy/ODN sensors, these authors have presumed it to be based either on the change of the capacitance/conductivity of the PPy/ODN film [**20**, **23**] or on the increase in the resistance to electron transfer by anions as a sequence of the negatively charged sugar phosphate backbone of the target DNA [**24**]. Nevertheless, from the data, especially from the atomic force microscope (AFM) measurements in this paper, the underlying mechanism of the hybridization signal transduction in the hybrid PPy/ODN nanocomposite film sensor seems to be deserved a re-clarified.

In this work, electrochemical cyclic voltammetry (CV) and atomic force microscope (AFM) have been used to monitor the electrochemical properties and morphological information of PPy/ODN film before and after hybridization in order to validate the mechanism of hybridization response. From the combination of the data of the two measurements, the present authors think that there is a steric effect derived from the hybridization event on the immediate interface of the PPy/ODN nanocomposite film that damps the ion flux penetrating through this interface, and thus induces the signal differentiation on the electrode electrochemical properties. Therefore, a simple process of cyclic voltammetry modulation on the ion flux and thus the steric effect on the hybrid PPy/ODN nanocomposite film can achieve the signal recognition of DNA hybridization; see the illustration in Fig. 1. As a hypothesis, a brief explanation is the following. When the ODN probes entrapped in the PPy film hybridize with the incoming complementary target sequences, they undergo a conformational change from single-stranded coiled states to relatively rigid double-stranded helix states. This conformational change somewhat twists the PPy backbone and the hybrid film network, thus leading to the formation of a more compact structure at the immediate interface between the polymer and solution – that is, the steric effect, which in turn hinders the ion flux penetrating into this interface during the redox process.

Through the validation of the above-mentioned hypothesis, and optimization of hybridization conditions on such hybrid PPy/ODN nanocomposite film sensor, it is argued that this work not only presents a new mechanism interpretation for PPy/ODN-based label-free DNA hybridization detection but also provides a simplified DNA sensor format convenient for practical applications.

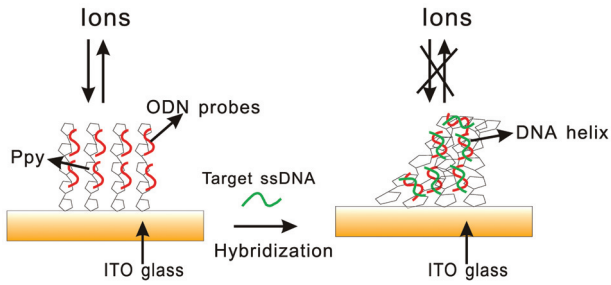

Fig. 1 Schematic illustration for the steric effect mechanism presented on the interface of hybrid PPy/ODN film after hybridization

Downloaded from pin.sagepub.com at NATIONAL UNIV SINGAPORE on August 7, 2011

2 MATERIALS AND METHODS

2.1 Reagents

Pyrrole monomer (chemical grade) was purchased from Sinopharm Chemical Reagent Co. Ltd (Shanghai, China) and was distilled until a colourless liquid was obtained. It was stored in a refrigerator before use. The following custom oligonucleotides, specific to *variola major* virus, were purchased from Shenggong Bioengineering Ltd (Shanghai, China): probe (P1): 20-mer 5'-GCAATAGTAATCAGGTAGAG-3'; the complementary target oligonucleotides (C1): 5'-CTCTACCTGATTACTATTGC-3' and the non-complementary control which has the same sequence as the probe sequence P1. The stock solutions for oligonucleotides were prepared in ultrapure water with Millipore system (18.2 MΩ) and stored at a temperature of –20 °C prior to use. The phosphate buffered saline (PBS: 137 nM NaCl, 2.7 mM KCl, 10 mM Na_2HPO_4, 2 mM KH_2PO_4), PH 7.4, was prepared with analytical grade reagents in MiliQ water. Other reagents were used under common conditions, unless specified.

2.2 Experimental equipment

Electropolymerization and electrochemical detection experiments were realized by cyclic voltammetry in a home-made micro-electrochemical cell (internal volume 100 μl) with indium tin oxide (ITO)-coated glass (which had a surface resistivity of 95 Ω/square) as a working electrode (area of 0.49 cm^2), a platinum wire coil as an auxiliary electrode, and a Ag/AgCl wire as a reference electrode. All electrochemical experiments were performed in a CHI-800 electrochemical workstation (Shanghai Chenhua Ltd, Shanghai, China). Electrochemical electropolymerization solution was thoroughly deoxygenated by N_2 bubbling for 5 min before use. In addition, AFM images were obtained by a CSPM 5000 system (Ben Yuan Ltd, Beijing, China). The quantity of ODN immobilization was characterized with a micro-spectrophotometer (K5500, Kaiao Technology Development Co. Ltd, Beijing, China).

2.3 Pyrrole electropolymerization and probe immobilization

The immobilization of ODN probes within polypyrrole film was realized by an in-situ entrapment route in which the ODN probes acted as the sole dopant during the growth of PPy film on the electrode surface. Nitrogen-bubbled electropolymerization monomer solution of 100 μL containing 0.1M pyrrole monomer and 1×10^{-5} M oligonucleotide (P1) was injected into the electrochemical cell to obtain ODN/PPy composite film on the ITO electrode surface by a continuous cyclic voltammtric scanning between 0.0 and +0.70 V (versus Ag/AgCl) with 20 mV s^{-1} scan rate. The amount of ODN probe molecules immobilized into the PPy film was quantified spectrophotometrically by comparing the OD_{260} of electopolymerization solution before and after the polymerization process. Before electropolymerization, the ITO-glass was successively cleaned by ultra-sonication in acetone, ethanol and deionized water for 5 min respectively, and then dried by nitrogen steam. The resulting PPy/ODN nanocomposite film was characterized by cyclic voltammetry (CV) and AFM in tapping mode (240 μm-long tetrahedral silicon cantilever with 2 N/m spring constant, from Olympus, Japan).

2.4 Hybridization and electrochemical detection

Before hybridization, CV was applied to characterize the PPy/ODN film modified ITO electrode between −0.40 to 0.40 V (versus Ag/AgCl) in PBS solution with 50 mV s^{-1} scan rate at room temperature. After that, hybridization reaction was done by exposing the PPy/ODN nanocomposite-film-modified ITO electrode in the 100 μL PBS buffer contained with the non-complementary oligonucleotide (1.0×10^{-6} M) for 1 h at 38 °C. After washing, CVs were recorded for evaluating any nonspecific interaction. In the following, the PPy/ODN electrodes, which were prepared with the same process, were incubated at the same PBS solutions containing different concentrations of complementary target DNA (from 1.0×10^{-18} M – 1.0×10^{-10} M) for 1 h at 38 °C. After that, the electrode was washed three times by PBS buffer solution to remove the unhybridized oligonucleotides, and then CVs were recorded again for electrochemical investigation of the hybridization reaction similar to the characterizing procedure of PPy/ODN before hybridization in the same PBS solution. Unless otherwise stated, all electrochemical measurements were performed at room temperature and registered until complete stabilization of the CV signals. The last scan was taken into consideration and analysed by ORIGIN 7.0 software (Micro Software, Northampton, MA).

3 RESULTS AND DISCUSSION

3.1 Preparation of the PPy/ODN film

The hybrid PPy/ODN nanocomposite film was prepared on the electrode surface by doping the ODN probes within the electro-polymerized PPy, in which

Downloaded from pin.sagepub.com at NATIONAL UNIV SINGAPORE on August 7, 2011

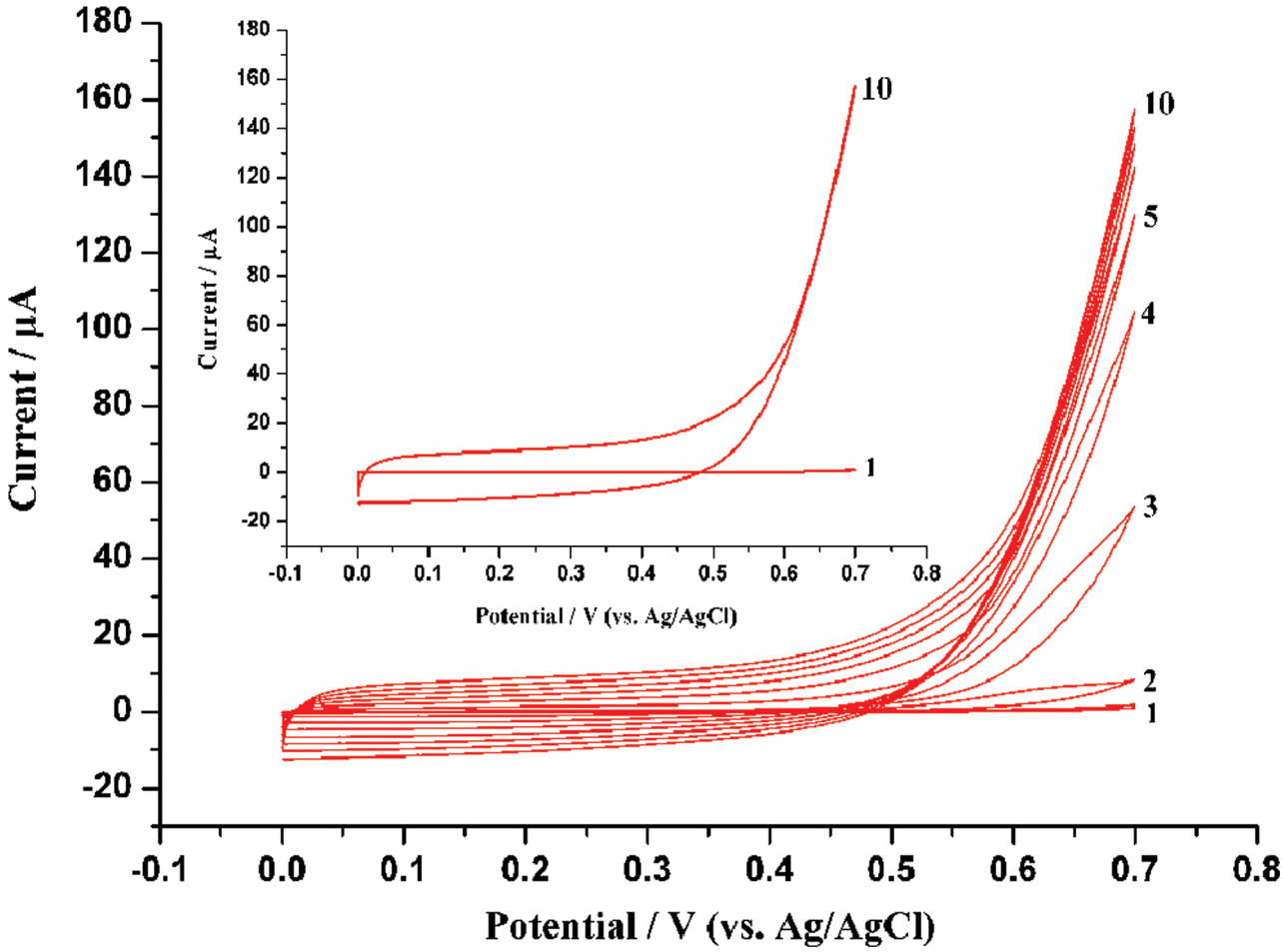

Fig. 2 Repetitive cyclic voltammograms for PPy electropolymerization on ITO electrode surface in a polymerization solution containing 0.1 M pyrrole monomer and 1×10^{-5} M ODN probe (P1) between 0.0 and 0.7 V(versus Ag/AgCl) at 20 mV s^{-1} for ten cycles. Inset: the first and tenth cycles

these probes acted as the sole counter ions during the growth of the conducting film. Thus-formed film could be considered as an efficient interface between the nucleic acid recognition system and the electrochemical transducer system. The electropolymerization of the PPy/ODN nanocomposite film can be conducted by cyclic voltammetry or constant potential [**23**]. In this paper, the desired ODN probe was immobilized on the ITO electrode surface by an adaptation of the methods described first by Wang and co-workers [**20**], taking the optimized parameters of Komarova *et al.* [**23**] into consideration. It has been proved that 20-30-mer long ODNs can serve as sole charge-compensating counter-ions during the electropolymerization of polypyrrole and that the incorporation behaviour of ODN molecules is similar to that of small inorganic anions. In this way, the oligonucleotide has a maximum possible incorporation in the conductive polymer and does not undergo any redox damage in the potential range used for electropolymerization. In addition, ODNs attached to the polypyrrole by their phosphate backbone, and the nucleotide bases are exposed to the solution and still retain their specific hybridization activity [**24**].

Figure 2 displays the repetitive cyclic voltammograms recorded during the electroploymerization of PPy onto ITO electrode surface in the presence of 1×10^{-5} M ODN probe (P1) between 0.0V to 0.7V with 20 mV s^{-1} scan rate for ten cycles. The increasing current response observed in the electrolyte-free ODN solution upon repetitive cycling suggests an efficient film growth [**21**, **25**]. Such a profile indicates that the anionic ODNs are effectively incorporated within the growing film for maintaining its electrical neutrality in a manner analogous to the doping of PPy by other anionic macromolecules [**21**]. In addition, the growth of the polypyrrole

Downloaded from pin.sagepub.com at NATIONAL UNIV SINGAPORE on August 7, 2011

continues with the number of sweepings and in the course of successive cycles monomer oxidation occurs at less and less positive potential (inset of Fig. 1). This change might contribute to the fact that there was gradual decrease in the nucleation and growth energy for PPy polymerization as the PPy/ODN nanocomposite gradually formed per cycle.

To characterize the ODN probe entrapped within the PPy, AFM was first used to obtain the morphologic information of the prepared PPy/ODN by tapping mode at a $2\,\mu m \times 2\,\mu m$ scale with 2 Hz scan frequency. In contrast, PPy/Cl film electropolymerized in a solution containing 0.1M pyrrole monomer and 0.1M NaCl was also subjected to the same method as a control. Figure 3(a) shows an AFM image of PPy/Cl film electropolymerized on the ITO electrode surface, while Fig. 3(b) shows an AFM image of PPy film entrapped with the desired 20-mer ODN probes. From Fig. 3, it can be inferred that the PPy films were constructed by overlapping of PPy particles with 43.8 nm average diameter. Importantly, there appeared some thin-coiled flocks randomly around the PPy particles seen in Fig. 3(b). This phenomenon leads to the result that the PPy/ODN has a smoother surface with a surface roughness of 3.13 nm (root mean square, RMS) than that of PPy/Cl with a surface roughness of 5.47nm RMS. It is argued by the present authors that the coiled flocks presented on the surface of PPy film could be ODN probes. More importantly, the visualization of ODN probes confirmed that part of the ODN probes immobilized by this approach still present their complementary ability to their target DNA sequences.

The preparation reproducibility of the PPy/ODN nanocomposite film was tested by the electrochemical activity of the resulted film measured by CV. The degree of its reproducibility was estimated based on the data derived from the area under the cyclic voltammogram. The preparations of PPy/ODN were conducted at different times ($n = 6$), and resulted in an average CV area of 85.46 μC with standard deviation (SD) of 5.53 μC and relative standard deviation (RSD) of 6.47 per cent. In addition, the quality of the ODN probes entrapped in the polypyrrole was determined by measuring the concentration of ODN in the polymerization solution before and after the electrodeposition process with a spectrophotometer, and the result was 0.72 nmole with SD = 0.08 nmole and RSD = 11.11 per cent.

3.2 DNA hybridization and its hindrance effect to ion exchange kinetics

The DNA hybridization event occurring on the prepared PPy/ODN nanocomposite film electrode and its hindrance mechanism could be differentiated by means of the combination of CV [**26**] and AFM.

Figure 4(a) shows the cyclic voltammograms of PPy/ODN nanocomposite film obtained before and after hybridization. Cyclic voltammogram a was the result of the PPy/ODN nanocomposite film in PBS solution before hybridization; cyclic voltammogram b shows the result of the PPy/ODN nanocomposite film again in the same PBS buffer after incubation within non-complementary target ssDNA solution for 1 h. No significant difference between these voltammograms was obtained. Then the PPy/ODN nanocomposite film coated ITO electrode was hybridized with the complementary target for 1 h and, after washing, the cyclic voltammogram (c) was recorded. Comparing the cyclic voltammograms a and c, a significant diminishment of area under the cyclic voltammograms can be noted, which is closely related to the ion-exchange kinetics of PPy/ODN nanocomposite film during the redox process.

Why this result? First, it should be mentioned that the amount of DNA strands with negative charge in the PPy/ODN nanocomposite film electrode increased with the inflowing of target DNA strands after hybridization. This is the only observable fact in the case of the PPy/ODN sensing system. Therefore, the immediate question is how the addition of target DNA strands could lead to the significant decreasing of area under the cyclic voltammogram.

Does the electrostatic effect from the incoming negative charges lead to the decrease of the ion-exchange kinetics between the PPy/ODN nanocomposite film and solution? The present authors noted that the entrapped ODN could not be readily expelled from the PPy network under CV cycle as the ODN probe could be considered as large dopants [**21**]; thus, the hybridized double-strand DNA (dsDNA) in the PPy network did also. As a result, the movement of the electrolytic cation, which follows

$$\mathrm{PPy(dsDNA^{n-})_x(Na^+)_{nx}} \rightarrow \mathrm{PPy^{x+}(dsDNA^{n-})_x} + \mathrm{nxNa} + + \mathrm{nxe^-}$$

dominates the electrochemically controlled ion-exchange behaviour of the hybridized PPy/ODN nanocomposite film. Therefore, the addition of negative charges by hybridization should not have a positive effect on the diminishment of cation exchange kinetic. Therefore, the electrostatic effect could not be the main factor for the diminishment in the ion-exchanging kinetics.

Moreover, it was noted, when comparing cyclic voltammograms a and b in Fig. 4(a) more carefully, that the area under cyclic voltammogram b is larger

Downloaded from pin.sagepub.com at NATIONAL UNIV SINGAPORE on August 7, 2011

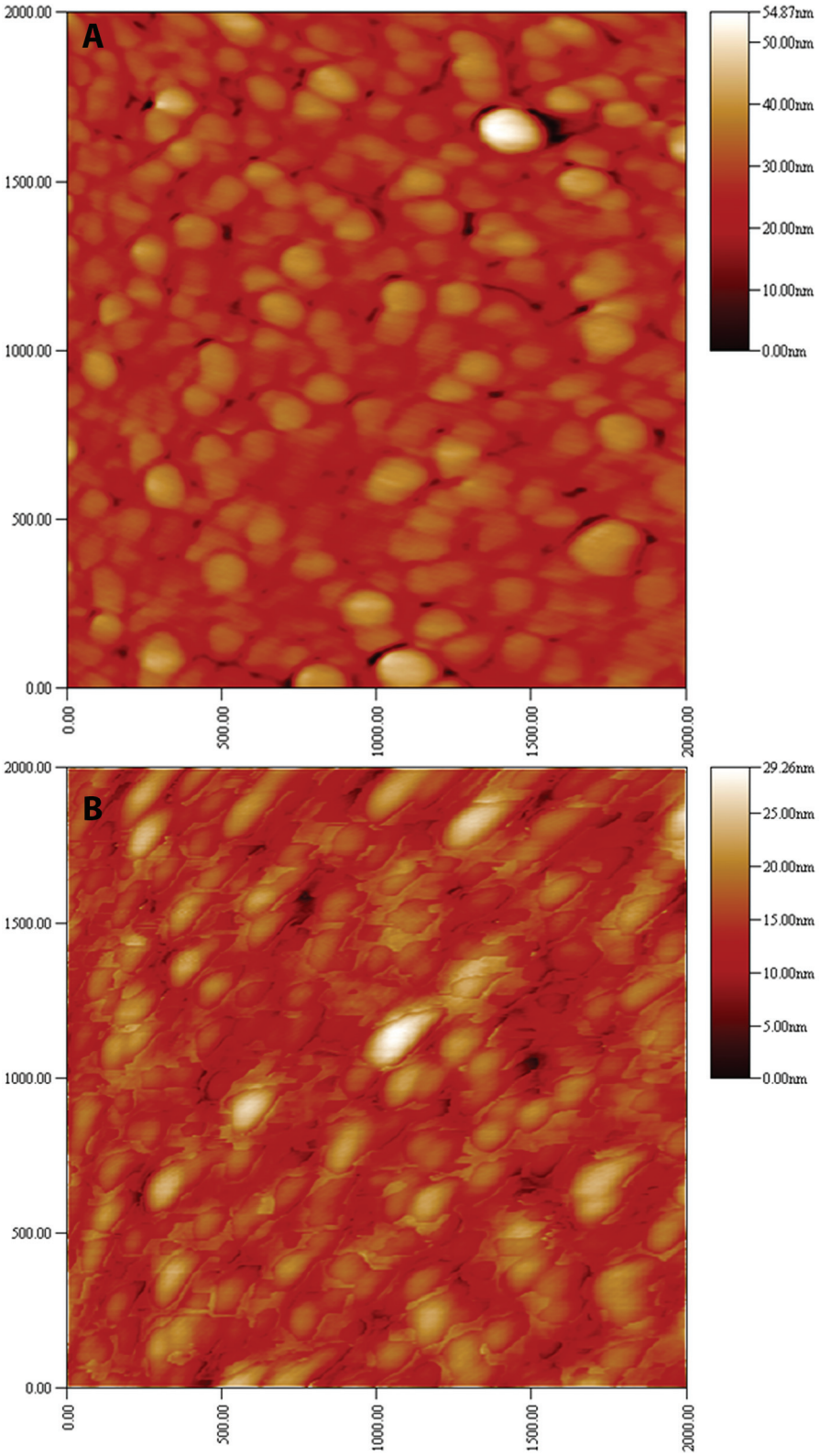

Fig. 3 AFM images of polypyrrole electropolymerization on ITO electrode surface by cyclic voltammetry between 0.0–0.7 V (versus Ag/AgCl) for ten cylices with a 20 mV s^{-1} scan rate in the polymerization solution containing (a) 0.1M pyrrole monomer and 1.0 M NaCl and (b) 0.1 M pyrrole monomer and 1×10^{-5} M ODN probe

Downloaded from pin.sagepub.com at NATIONAL UNIV SINGAPORE on August 7, 2011

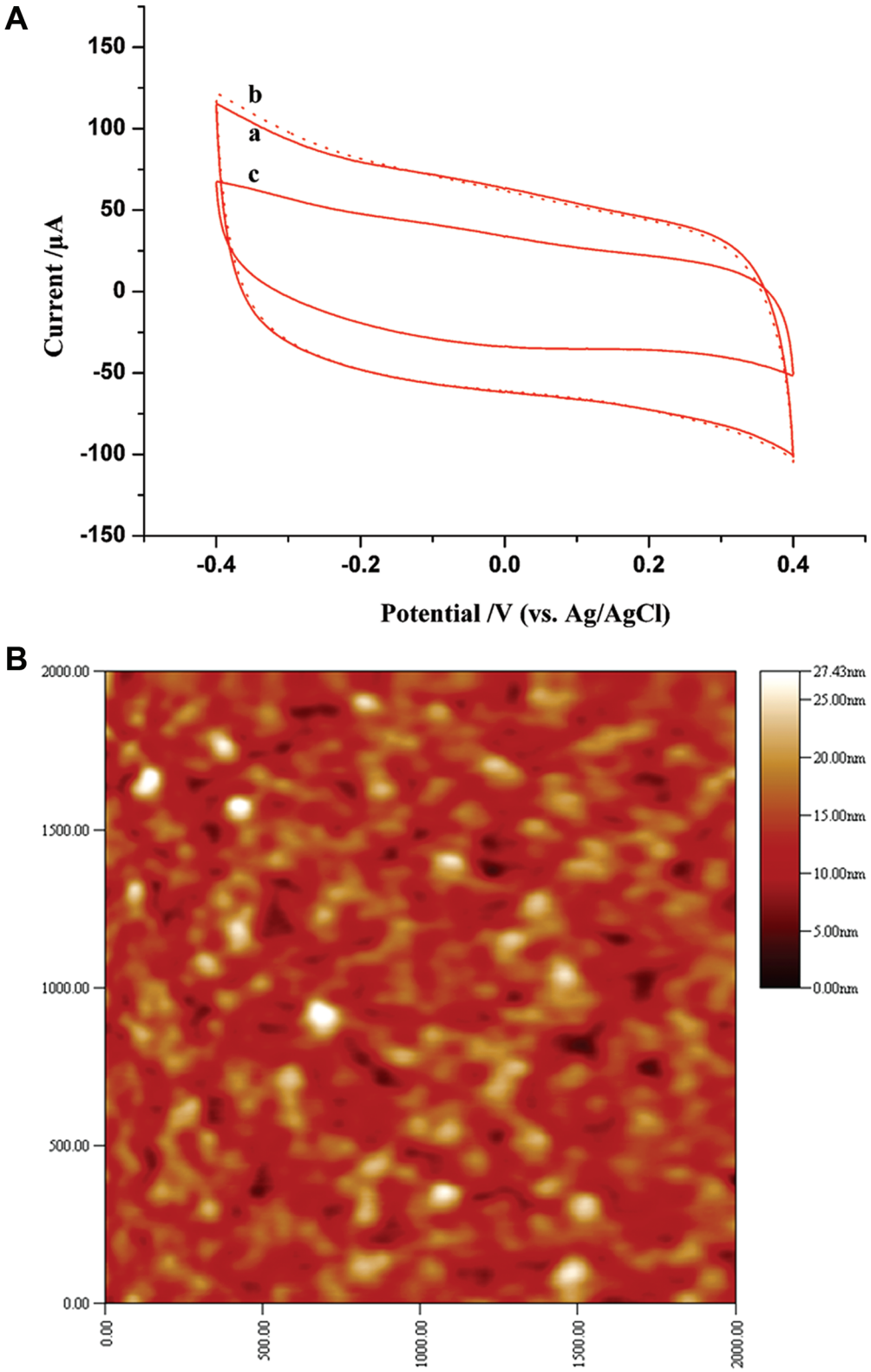

Fig. 4 (a) Cyclic voltammograms recorded in PBS buffer solution between –0.4 V and 0.4 V (versus Ag/AgCl) at a scan rate of 50 mv/s: curve a, CV of the PPy/ODN film before hybridization; curve b, CV of the same film as in curve a but in response to exposure to a 1×10^{-6} M non-complementary target ssDNA for 1 h; curve c, CV response of the same film as in curve (a) after hybridization with 1×10^{-6} M complementary target ssDNA for 1 h. The PPy/ODN was prepared by 10 cycles. (B) AFM image of PPy/ODN film after hybridization with 1×10^{-6} M complementary target DNA for 1 h at 37 °C in PBS solution

Downloaded from pin.sagepub.com at NATIONAL UNIV SINGAPORE on August 7, 2011

than that of cyclic voltammogram a by 7.2 per cent, which means an enhancement of ion exchanging kinetic after incubation with non-complementary target. This might be due to the increase of the polymer's conductivity by the doping of non-complementary ssDNA which adsorbed on the PPy/ODN nanocomposite film non-specifically [**24**]. This opposite signal appearance is similar to the result reported by Wang *et al.* [**20**] and Komarova *et al.* [**23**]. Recently, Tosar *et al.* also found that the amplitude of PPy oxidation and reduction decreases after hybridization with complementary target, while it increases after incubation with a non-complementary target [**24**]. They explained this by the above-mentioned electrostatic effect, that the decrease in PPy peak contributed to the increase in the resistance of electron transfer by electrostatic repulsing towards anion incorporation, while the increase in PPy peaks was due to increase in conduction of PPy by doping. This point remains to be confirmed.

Taking into account also the data from AFM, it is argued that there could be some hindrance effect on the cation exchange kinetic, occurring immediately after hybridization at the interface between PPy/ODN and the solution under electrochemical CV process. The existence of a hindrance barrier could explain why the ion exchange kinetic is slowed down by hybridization. For validation, AFM was used again to characterize the morphological changes in PPy/ODN after hybridization. Figure 4(b) shows the AFM image of PPy/ODN nanocomposite film on ITO electrode after hybridization. Comparing the AFM images of Figs 3(b) and 4(b), it is clear that a significant morphological change has occurred. Before hybridization (Fig. 3(b)), the PPy/ODN nanocomposite film shows a relatively ordered and flat structure, while after hybridization (Fig. 4(b)), the surface structure of the PPy/ODN nanocomposite film has become more rugged – the flocks have become roughened, twisted, and entangled. Such a compact topography could be assumed as an important consequence in the formation of hindrance layer for ion exchanging and transport. This result is similar to that of a quinine-based DNA sensor reported by Reisberg *et al.* [**27**, **28**], in which an ODN probe was absorbed on the surface of a conducting polymer. To further ask why there could be the formation of such a hindrance, the present authors' explanation is that there may be a large amount of steric effects induced by molecular conformational changes in the PPy/ODN film, which is the determinant factor in the electrochemical response, and meanwhile the electrostatic effect is negligible.

3.3 Influence of the PPy/ODN film thickness on DNA hybridization detection

Obviously, due to the existence of the hindrance effect, the sensing performance of PPy/ODN nanocomposite film is influenced by the thickness of the polymer film. Here, the sensitivity of hybridization detection was tested as a function of the thickness of

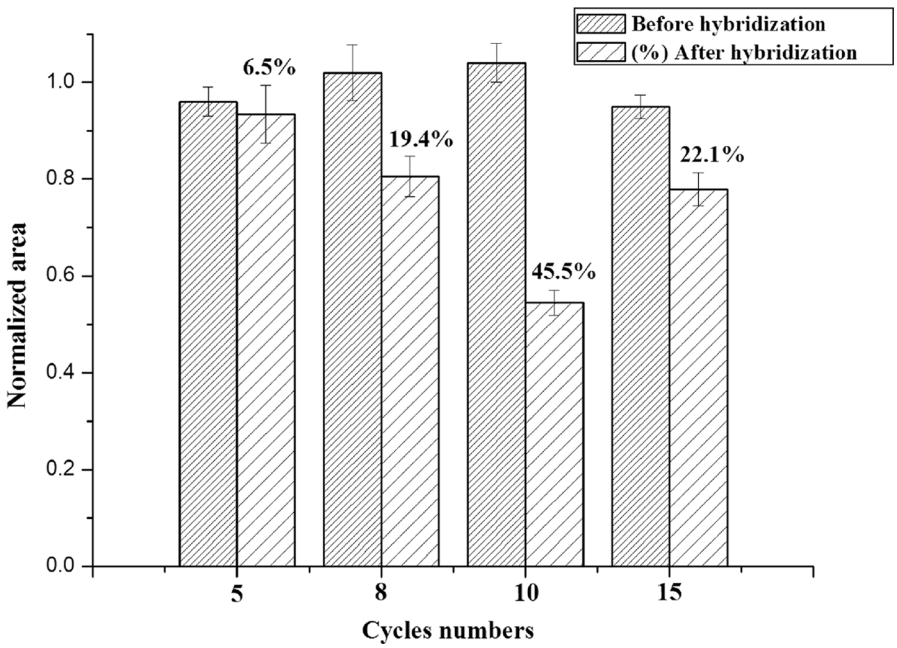

Fig. 5 Histograms derived from the diminishment percentage of the normalized area under the CVs of PPy/ODN film between the initial state and after hybridization for different thickness conditions. The error bars are derived form three experiments ($n = 3$)

Downloaded from pin.sagepub.com at NATIONAL UNIV SINGAPORE on August 7, 2011

the polymer film. Figure 5 shows the histograms derived from the areas under the cyclic voltammograms obtained before and after hybridization by adjusting the number of the cyclic voltammetric cycle (5 cycles, 8 cycles, 10 cycles, and 15 cycles) for the PPy/ODN film electropolymerization. The decrease in percentage was calculated by comparing the area under CV recorded before hybridization (this value is set as 100 per cent) and the ones obtained after subtraction of the hybridized state (curve c in Fig. 3(a)) from the initial state (curve a in Fig. 3(a)). For thin films, only a small decrease in the signal was observed (6.5 per cent, 5 cycles), which become more pronounced at eight cycles (19.4 per cent). The optimum response for DNA hybridization detection has been observed at 10 cycles, which corresponds to a 45.5 per cent decrease compared to that before hybridization. However, if the thickness of PPy/ODN is increased to 15 cycles, the response of hybridization detection decreases to 22.1 per cent, which suggests a weaker affinity of the ODN probe to the target DNA for a thicker film. The result is very different from that of the previous report that thinner PPy/ODN nanocomposite film showed a better response [**23**]. This performance may be a composite effect of the electrochemical activity of PPy and the affinity of ODN probes to target DNA. Whatever the case, ten cycles were chosen as the optimum thickness for PPy/ODN electropolymerization.

3.4 Effect of incubation time on hybridization detection

Figure 6 shows the influence of the hybridization time (0 min to 80 min with a 10 min interval) on the electrochemical response of DNA hybridization detection. From Fig. 6 it can be seen that the response of the sensor initially increases significantly with the increase of time until 60 min, which corresponds to a 45.5 per cent decrease in the area of cyclic voltammogram compared with that of before hybridization (the value set as 100 per cent), and increases slowly from 60 min to 80 min. In this case, the difference between the analytical signals recorded at the 60th and 80th minute of incubation time did not exceed 1 per cent, indicating that the hybridization reaction was dominantly completed after 60 min. Considering the sensitivity and assay time, therefore, 60 min was chosen as the hybridization time in this work.

4 SENSING SENSITIVITY

Under the above proposed optimization conditions (10 cycles for PPy/ODN prepared, hybridization

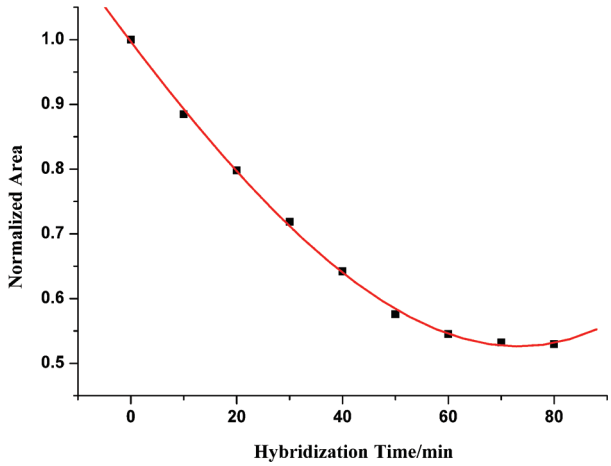

Fig. 6 The influence of hybridization time on the response for DNA hybridization detection. The curve was derived form the areas under the CVs of the PPy/ODN film hybridized with complementary target at different time after normalized with that of before hybridization (this value set as 100 per cent). Other conditions were as the same as Fig. 4(a)

time was chosen for 1 h), the analytical performance of the DNA hybridization detection was investigated. Figure 7(a) shows the cyclic voltammograms of PPy/ODN film after hybridization with different concentrations of target DNA from 1×10^{-18} M to 1×10^{-10} M. From Fig. 7(a) it can be seen that the areas under the cyclic voltammograms decreased with the increase of target DNA concentration. As explained previously, the hybridization reaction between the ODN probes entrapped within PPy film and the complementary target DNA could induce the structure of PPy/ODN nanocomposite film to be more twisted and compact, which in turn hinders the electrochemically controlled cation exchange kinetic between the PPy/ODN nanocomposite film and solution by steric effect. The slowdown of ion exchanging kinetic corresponded to the decreased area under the cyclic voltammogram when compared to that before hybridization. It is reasonable to argue that the increases in hybridization will further decrease the area under the cyclic voltammogram. Figure 7(b) shows the calibration curve of the areas under the cyclic voltammograms in Fig. 7(a) (normalized by the area under the cyclic voltammogram of PPy/ODN before hybridization) against the logarithm of the concentration of target DNA in the range from 1×10^{-18} M to 1×10^{-10} M. Each concentration was repeated three times. It can be noted that the signal levelled off above 1×10^{-10} M., reflecting that the probe hybridization sites available were as low as 10 fmole. Furthermore, the normalized

Downloaded from pin.sagepub.com at NATIONAL UNIV SINGAPORE on August 7, 2011

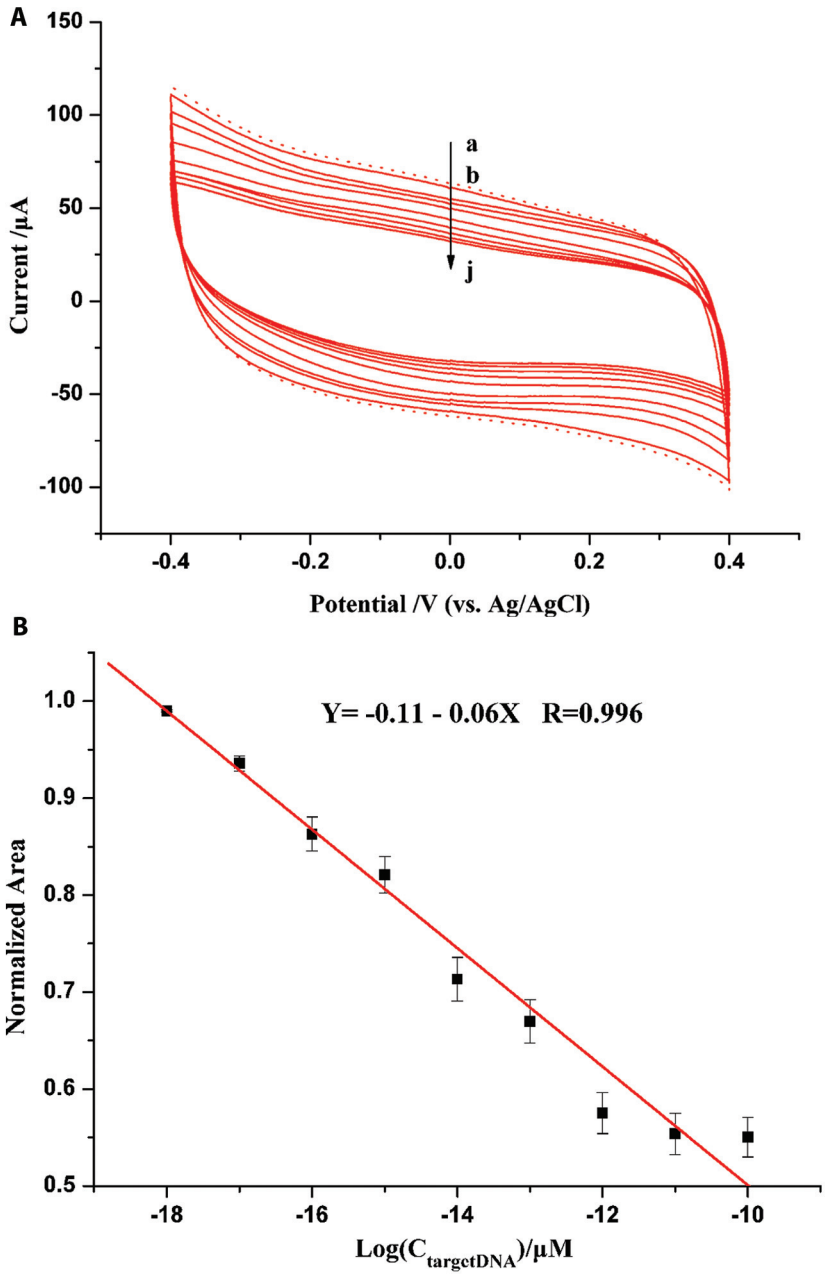

Fig. 7 (a) The CVs of PPy/ODN before (location a) and after hybridization with different concentrations of the complementary target DNA from 1×10^{-18} M to 1×10^{-10} M with a 10 M interval (corresponding to b–j CV, respectively). (b) The calibration curves for the normalized area under the CVs against the target concentration in the range from 1×10^{-18} M to 1×10^{-10} M. Each concentration was recorded in three times ($n=3$)

area is linear with the logarithm of the concentration of the complementary target DNA. The linear regression equation was $Y=-0.11-0.06X$, where Y is the normalized area derived from the integral of the CVs, while X represents the log C (unit of C is M), and the correlation coefficient (R) was 0.996. The detection limit of the DNA biosensor was 5×10^{-18} M target DNA. In this case, the normalized area changed after 60 min incubation with the complementary ssDNA sequence was 0.072, which is three times the normalized area change of 0.024 calculated for the same electrode incubated in blank PBS buffer. The detection limit of the proposed electrochemical detection of DNA hybridization is superior to that reported by Peng *et al.* [**29**] and Chang *et al.* [**30**], who amplified the hybridization signal by nanoparticles (~1n*M*) and by layer-by-layer technique (3.2×10^{-14} M) respectively. This proposed approach has a detection limit as small as 10^{-18} M, which is typically required for medical

Downloaded from pin.sagepub.com at NATIONAL UNIV SINGAPORE on August 7, 2011

diagnostic application [**31**], though the detection linear range in this proposed method was lower.

5 CONCLUSIONS

An underlying mechanism attributing to the steric effect for the interpretation of hybridization discrimination on the hybrid PPy/ODN nanocomposite film, as a simply-enough electrochemical sensor for label-free DNA hybridization, was presented and proven by the technical combination of cyclic voltammetry and AFM measurements. Upon hybridization with complementary target DNA, the PPy/ODN nanocomposite film undergoes a morphologic change, becomes more compact and twisted, which in turn diminishes the electrochemically controlled cation exchange kinetic between the PPy/ODN and buffer solution. This whole behaviour could obviously be a steric effect in the hybridization signalling discrimination. A label-free electrochemical DNA biosensor based on this hybrid PPy/ODN nanocomposite film on ITO electrode was constructed and optimized to evaluate its detection ability. It was found that a low detection limit of 5×10^{-18} M could be achieved. This work gives the authors a chance towards a better understanding of this attractive PPy/ODN biosensing composite and a further basis for the development of label-free DNA sensor using the simple-enough hybrid film of PPy/ODN.

FUNDING

This paper was supported by the Key Project for International Science and Technology Collaboration of the Ministry of Science and Technology (2005DFA00190) and by an NSFC grant (30870607), a CSTC grant (2008BB5192), and the '111 Project' (B06023).

© Chongqing University 2011

REFERENCES

1 **Li, J., Wei, W. Z.,** and **Luo, S. L.** A novel one-step electrochemical codeposition of carbon nanotubes-DNA hybrids and tiron doped polypyrrole for selective and sensitive determination of dopamine. *Microchimica Acta*, 2010, **171**(1–2), 109–116.

2 **Wang, J.** Electrochemical nucleic acid biosensors. *Anal. Chim. Acta*, 2002, **469**, 63–71.

3 **Wang, J.** Towards genoelectronics: electrochemical biosensing of DNA hybridization. *Chem. Eur. J.*, 1999, **5**, 1681–1685.

4 **Hashimoto, K., Ito, K.,** and **Ishimori, Y. S.** Microfabricated disposable DNA sensor for detection of hepatitis B virus DNA. *Sens. Actuators B*, 1998, **46**, 220–225.

5 **Yan, F., Erdem, A., Meric, B., Kerman, K., Ozsoz, M.,** and **Sadik, O. A.** Electrochemical DNA biosensor for the detection of specific gene related to Microcystis species. *Electrochem. Commun.*, 2001, **3**, 224–228.

6 **Carpini, G., Fausto, L., Giovanna, M.,** and **Mascini, M.** Oligonucleotide-modified screen-printed gold electrodes for enzyme-amplified sensing of nucleic acids. *Biosens. Bioelectron.*, 2004, **20**, 167–175.

7 **Takenaka, S., Yamashita, K., Takagi, M., Uto, Y.,** and **Kondo, H.** DNA sensing on a DNA probe-modified electrode using ferrocenyl naphthalene diimide as the electrochemically active ligand. *Anal. Chem.*, 2000, **72**, 1334–1341.

8 **Wang, J., Liu, G.,** and **Merkoci, A.** Electrochemical coding technology for simultaneous detection of multiple DNA targets. *J. Am. Chem. Soc.*, 2003, **125**, 3214–3215.

9 **Cao, Y. C., Jin, R.,** and **Mirkin, C. A.** Nanoparticles with Raman spectroscopic fingerprints for DNA and RNA detection. *Science*, 2002, **297**, 1536–1540.

10 **Bolívar, P. H., Nagel, M., Richter, F., Brucherseifer, M., Kurz, H., Bosserhoff, A.,** and **Büttner, R.** Label-free THz sensing of genetic sequences: towards 'THz biochips'. *Phil. Trans. R. Soc. London A*, 2004, **362**, 323–335.

11 **Daniels, J. S.** and **Pourmand, N.** Label-free impedance biosensors: opportunities and challenges. *Electroanalysis*, 2007, **19**, 1239–1257.

12 **Ramanaviciene, A.** and **Ramanavicius, A.** Pulsed amperometric detection of DNA with an ssDNA / polypyrrole-modified electrode. *Anal. Bioanal. Chem.*, 2004, **379**, 287–293.

13 **Wang, J., Jiang, M., Fortes, A.,** and **Mukherjee, B.** New label-free DNA recognition based on doping nucleic-acid probes within conducting polymer films. *Anal. Chim. Acta*, 1999, **402**, 7–12.

14 **Cai, H., Xu, Y., He, P. G.,** and **Fang, Y. Z.** Indicator free DNA hybridization detection by impedance measurement based on the DNA-doped conducting polymer film formed on the carbon nanotube modified electrode. *Electroanalysis*, 2003, **15**, 1864–1869.

15 **Wang, J.** Review Electrochemical nucleic acid biosensors. *Anal. Chim. Acta*, 2002, **469**, 63–71.

16 **Francis, G., Hafsa, K. Y., Pratima, S., Bernard, M.,** and **Thierry, D.** Toward intelligent polymers: DNA sensors based on oligonucleotide-functionalized polypyrroles. *Synth. Met.*, 1999, **100**, 89–94.

17 **Chaker, T., Jaffrezic-Renault, N. J., Claude, M.,** and **Hafsa, K. Y.** Direct electrochemical probing of DNA hybridization on oligonucleotide-functionalized polypyrrole. *Mater. Sci. Engng C*, 2008, **28**, 848–854.

18 **Ghanbaria, K., Bathaieb, S. Z.,** and **Mousavi, M. F.** Electrochemically fabricated polypyrrole nanofiber-modified electrode as a new electrochemical DNA biosensor. *Biosens. Bioelectron.*, 2008, **23**, 1825–1831.

Downloaded from pin.sagepub.com at NATIONAL UNIV SINGAPORE on August 7, 2011

19 **Li, Y., Jiang, J. H., Ma, X. D., Dong, G. X., Wang, J.,** and **Paul Sung, K.-L.** Polypyrrole/oligonucleotide nanocomposite: its initial growth. *J. Nanoenging Nanosyst.*, 2008, **222**, 57–63.

20 **Wang, J., Jiang, M., Fortes, A.,** and **Mukherjee, B.** New label-free DNA recognition based on doping nucleic-acid probes within conducting polymer films. *Anal. Chim. Acta*, 1999, **402**, 7–12.

21 **Wang, J.** and **Jiang, M.** Toward genoelectronics: nucleic acid doped conducting polymers. *Langmuir*, 2000, **16**, 2269–2274.

22 **Xu, Y., Jiang, Y., Cai, H., He, P. G.,** and **Fang, Y. Z.** Electrochemical impedance detection of DNA hybridization based on the formation of M-DNA on polypyrrole/carbon nanotube modified electrode. *Anal. Chim. Acta*, 2004, **516**, 19–27.

23 **Komarova, E., Aldissi, M.,** and **Bogomolova, A.** Direct electrochemical sensor for fast reagent-free DNA detection. *Biosens. Bioelectron.,* 2005, **21**, 182–189.

24 **Tosar, J. P., Karen, K.,** and **Laiz, J.** Two independent label-free detection methods in one electrochemical DNA sensor. *Biosens. Bioelectron.,* 2009, **24**, 3036–3042.

25 **Eguiluz, K. I. B., Banda, G. R. S., Huacca, M. E. F., Alberice, J. V., Carrilho, E., Machado, S. A. S.,** and **Avaca, L. A.** Sequence-specific electrochemical detection of Alicyclobacillus acidoterrestris DNA using electroconductive polymer-modified fluorine tin oxide electrodes. *Analyst*, 2009, **134**, 314–319.

26 **Sadki, S., Schottland, P., Brodie, N.,** and **Sabouraud, G.** The mechanisms of pyrrole electropolymerization. *Chem. Soc. Rev.,* 2000, **29**, 283–293.

27 **Piro, B., Reisberg, S., Noel, V.,** and **Pham, M. C.** Investigations of the steric effect on electrochemical transduction in a quinone-based DNA sensor. *Biosens. Bioelectron.,* 2007, **22**, 3126–3131.

28 **Reisberg, S., Piro, B., Noel, V., Nguyen, T. D., Nielsen, P. E.,** and **Pham, M. C.** Investigations of the charge effect on electrochemical transduction in a quinone-based DNA sensor. *Eletrochim. Acta*, 2008, **54**, 346–351.

29 **Peng, H., Soeller, C., Cannell, M. B., Bowmaker, G. A., Cooney, R. P.,** and **Sejdic, J. T.** Electrochemical detection of DNA hybridization amplified by nanoparticles. *Biosens. Bioelectron.*, 2006, **21**, 1727–1736.

30 **Chang, Z., Chen, M., Fan, H., Zhao, K., Zhuang, S. Q., He, P. G.,** and **Fang, Y. Z.** Multilayer membranes via layer-by-layer deposition of PDDA and DNA with Au nanoparticles as tags for DNA biosensing. *Electrochim. Acta*, 2008, **53**, 2939–2945.

31 **Serge, C.** and **Pascal, M.** Recent advances in DNA sensors. *Analyst*, 2008, **133**, 984–991.

Downloaded from pin.sagepub.com at NATIONAL UNIV SINGAPORE on August 7, 2011